Inorganic Chemistry

Article

pubs.acs.org/IC

Cross-Linking the Fibers of Supramolecular Gels Formed from a Tripodal Terpyridine Derived Ligand with d-Block Metal Ions

Oxana Kotova,[†] Ronan Daly,[‡] Cidália M. G. dos Santos,[†,⊥] Paul E. Kruger,[§] John J. Boland,[∥] and Thorfinnur Gunnlaugsson*[,†]

[†]School of Chemistry, Trinity Biomedical Sciences Institute (TBSI), University of Dublin, Trinity College Dublin, Dublin 2, Ireland

[‡]Department of Engineering, University of Cambridge, Charles Babbage Road, Cambridge CB3 0FS, United Kingdom

[§]MacDiarmid Institute for Advanced Materials and Nanotechnology, Department of Chemistry, University of Canterbury, Private Bag 4800, Christchurch 8041, New Zealand

[∥]School of Chemistry, Centre for Research on Adaptive Nanostructures and Nanodevices (CRANN), University of Dublin, Trinity College Dublin, Dublin 2, Ireland

Supporting Information

ABSTRACT: The tripodal terpyridine ligand, **L**, forms 1D helical supramolecular polymers/gels in H_2O–CH_3OH solution mediated through hydrogen bonding and π–π interactions. These gels further cross-link into 3D supramolecular metallogels with a range of metal ions (**M**) such as Fe(II), Ni(II), Cu(II), Zn(II), and Ru(III); the cross-linking resulting in the formation of colored or colorless gels. The fibrous morphology of these gels was confirmed using scanning electron microscopy (SEM); while the self-assembly processes between **L** and **M** were investigated by absorbance and emission spectroscopy from which their binding constants were determined by using a nonlinear regression analysis.

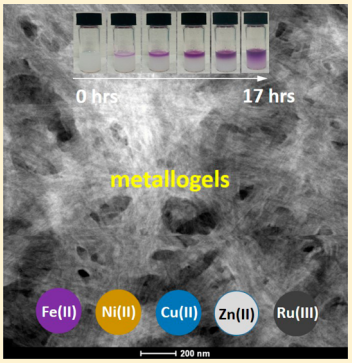

INTRODUCTION

While the concept of forming molecular gels from low-molecular weight compounds (gelators) was established more than a century ago,[1a] the focus over the past 20 years has been on broadening the scope of application of functional gels. It was found that the formation of gels as coordination polymers[1b] can be achieved by using small molecules without long chain hydrophobic groups that also possess fluorescence enhancement upon polymerization useful for a wide range of optical applications.[2a] In addition, such gels provide a viable route to obtain new crystal forms,[2b] enable encapsulation,[2c] and act as anion-responsive soft materials[2d] with rheological properties strengthened by the presence of nanoparticles.[2e] In turn, widening the scope of applications for low-molecular weight gelators led to a better understanding of gel formation,[3a−e] which was found to be mainly driven by self-assembly processes that take advantage of weak interactions such as host−guest recognition, π–π stacking, and/or hydrogen bonding.[3f,g] Metal−ligand coordination has also recently become an important tool to facilitate the self-assembly of gels. Such gels, known as metallogels, are often found to be highly robust where various physical properties of the metal ions (**M**) can be capitalized upon within the coordination environment of the gel structure.[4] In our previous work,[5a] we showed that the C_3-symmetric tripodal ligand **L** (Figure 1), based on a benzene-1,3,5-tricarboxamide (BTA)[5b−d] core conjugated to three terpyridine (tpy) units via carboxamide spacers, can be used in the formation of transparent organogels or metallogels using lanthanide ions. These luminescent gels were also used as chemical nanogarden platforms for growing inorganic nanowires from salts such as NaCl and KCl.[5e] Recently, Jung et al. have also used **L** to induce a chiral arrangement of achiral Au nanoparticles[6a] and as an aggregation-induced probe for Zn(II).[6b] The tpy ligand in **L** is commonly used in inorganic coordination and supramolecular chemistry with f- and d-metal ions.[7] In the past we have used tpy-based ligands in the formation of mixed f−d supramolecular conjugates with both Fe(II) and Ru(II) metal ions.[8a,b] Our research group has also recently shown the formation of metallogels from a Ru(II) complex with 2,6-bis(1,2,3-triazol-4-yl)pyridine (btp) ligands.[8c,d]

During the past few years different research groups used the tpy unit as the building blocks for the development of metallo-supramolecular polymers with d-block ions. For example, Fe(II)-based systems were shown to have the potential for display applications as well as smart window development,[9a] while incorporation of Zn(II) and Cd(II) opens an avenue for the development of light harvesting, photovoltaic materials, as well as nonlinear optical devices.[9b−d] Changes in the ligand

Received: March 22, 2015
Published: July 29, 2015

DOI: 10.1021/acs.inorgchem.5b00626
Inorg. Chem. 2015, 54, 7735−7741

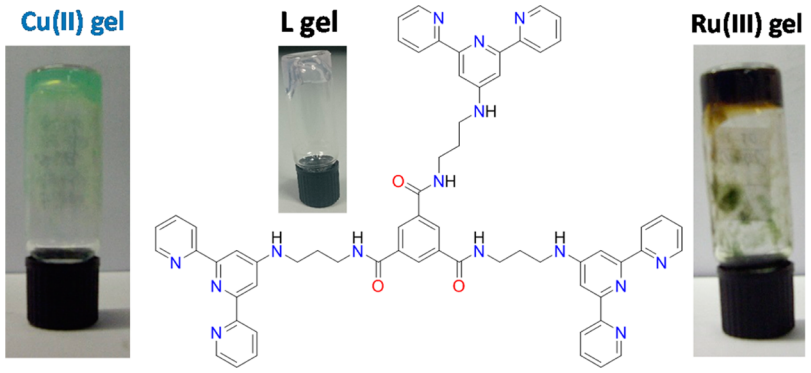

Figure 1. Tripodal ligand (**L**) used in the formation of metallogels with Fe(II), Ni(II), Cu(II), Zn(II), Ru(III).

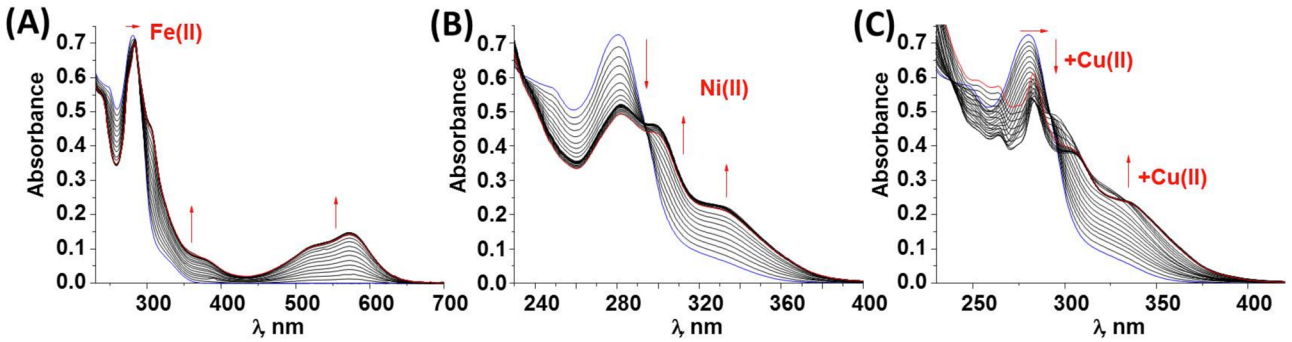

Figure 2. Changes in the absorbance spectrum of **L** ($c = 1 \times 10^{-5}$ M) with (A) Fe(II), (B) Ni(II), (C) Cu(II) (0 → 9 equiv) in methanol at 298 K. The arrows indicate the changes observed upon addition of increasing amounts of inorganic salts starting with the spectrum of the ligand only (blue —).

design as well as metal ion used helps to modify the resulting polymers including their rheological and morphological properties, as has been shown for Fe(II)-, Co(II)-, and Ru(II)-based supramolecular polymers[9e] as well as Ni(II)-based systems.[9f]

Herein, we examine the metal directed self-assembly formation and supramolecular gel formation of **L** with d-block metal ions such as Fe(II), Ni(II), Cu(II), Zn(II), and Ru(III) in dilute solution and at higher concentration within the gel-phase. The latter induces cross-linking between the fibers of the **L** gels with visible color changes.

RESULTS AND DISCUSSION

The formation of supramolecular polymers or metallogels with tpy-based molecules has proven benefits with established applications in fields such as sensing, etc.;[10,11] an area to which we have contributed in the past.[12] Having synthesized and characterized **L** we set out to investigate its self-assembly properties in CH_3OH solution ($c_L = 1 \times 10^{-5}$ M) with d-block ions by monitoring the changes in the ligand-centered absorbance and the fluorescence (Figure 2 and Supporting Information Figures S1–S8). The results showed that on all occasions these ions interacted with **L**. The main changes in the UV–vis absorption spectra occurred after the addition of 1 equiv (equiv) of Fe(II), Ni(II), or Zn(II), indicating the formation of the 1:1 (**M:L**) species at low concentration. The changes observed for the titrations of **L** with Ni(II) and Zn(II) are shown in Figure 2B and Supporting Information Figures S2, S3, S5, S6, respectively. In both cases, hypochromic shifts were observed for **L** in the $\pi \rightarrow \pi^*$ band centered at 280 nm with a hyperchromic shift observed for the 330 nm transition of **L**, assigned to tpy, an indication of coordination of **M** (Ni(II), Zn(II)) to tpy. The titration with Fe(II) also showed hypochromic shift for the 280 nm band and a hyperchromicity in the 330 nm transition of **L**. However, the characteristic formation of the metal-to-ligand charge transfer (MLCT) band with λ_{max} at 570 nm also emerged, indicating the complexation of Fe(II) to one or more of the tpy units in **L** (Figure 2A, Supporting Information Figure S1).[7] In the case of Cu(II) (Figures 2C and 3A), bands centered at 258, 280, and 283 nm,

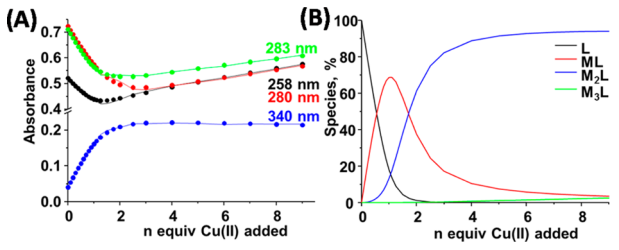

Figure 3. (A) Experimental binding isotherms (···) for the changes in the absorbance of **L** upon addition of Cu(II) and their corresponding fit (–). (B) Speciation-distribution diagram obtained from the fit.

all underwent hypochromic shifts up to the addition of 1 equiv of the metal ion. These changes were followed by less prominent decrease in the absorbance for the 280 and 283 nm bands up until addition of 3 equiv of Cu(II) after which an increase in the absorbance of these bands was observed. The band centered at 258 nm underwent hyperchromic shift upon addition of 1 → 9 equiv of Cu(II). In contrast, the band centered at 340 nm experienced hyperchromic shift upon addition of 0 → 2 equiv with the following formation of a plateau when 2 → 9 equiv of Cu(II) was added (Figure 3A).

DOI: 10.1021/acs.inorgchem.5b00626
Inorg. Chem. 2015, 54, 7735–7741

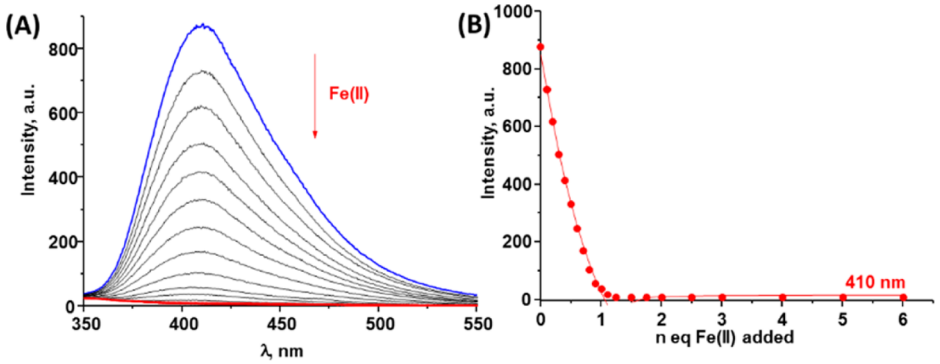

Figure 4. Changes in (A) the fluorescence spectrum of **L** ($c = 1.02 \times 10^{-5}$ M; $\lambda_{ex} = 280$ nm) upon addition of Fe(II) in methanol at 298 K with (B) the corresponding binding isotherm (red ···) and its fit (red —).

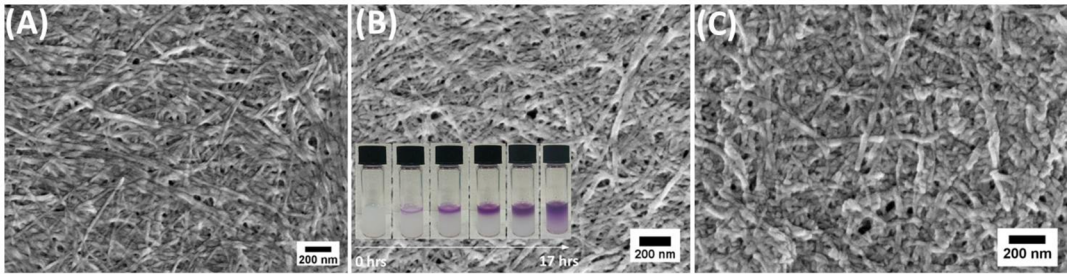

Figure 5. SEM images of (A) **L**, (B) Fe(II)-**L** (inset: diffusion of Fe(II) ions into the **L** gel over a period of 17 h), and (C) Zn(II)-**L** gels (scale bar corresponds to 200 nm). A very thin layer of gold/palladium was applied to enable imaging.

Taken in combination these results support the formation of 1:1, 2:1, and 3:1 **Cu:L** species in solution, and, hence, the use of **L** as a potential cross-linking center, where the d-block ions would function as a "supramolecular glue", bridging adjacent strands through interaction with the terminal tpy centers (Figure 3B). Ligand **L** was also titrated with Ru(III) (Supporting Information Figures S7,8). Here a two-step decrease was observed in the 280 nm absorption band with the first step occurring upon addition of 0 → 1 equiv of Ru(III) and the second step upon addition of 1 → 3 equiv of Ru(III). Simultaneously an increase in the 315 nm band occurred in two steps with the first step taking place upon addition of 0 → 1 equiv while the second one is at 1 → 3 equiv of Ru(III) ion added to the solution. Analysis of these changes showed the formation of both 1:1 and 3:1 **M:L** stoichiometries in solution, but no significant changes were observed for the 258 and 289 nm bands of **L** (see Supporting Information Figure S7). In all cases, the 1:1 **M:L** species shown above were also observed by MALDI MS (see Supporting Information Figures S9–S11). The emission properties of **L** were also investigated in the presence of these d-block metal ions. Excitation of **L** at 280 nm gave rise to ligand-centered fluorescence with $\lambda_{em} = 410$ nm. This emission was gradually quenched upon addition of 1 equiv of Fe(II), Cu(II) (100% quenching), Ni(II) (79% quenching), and Ru(III) (33% quenching) (see Figure 4, Supporting Information Figures S3, S4, S8), while for Zn(II) 85% emission enhancement was observed up to 1 equiv (Supporting Information Figure S6). The observed fluorescence quenching by metal ions such as Fe(II), Cu(II), Ni(II), and Ru(III) is a common phenomenon. These metals possess partially filled d-orbitals, and the decrease of ligand fluorescence upon addition of these ions can be explained by the quenching processes of the ligand excited states occurring through electron or energy transfer mechanisms.[13a,b] Unlike these metals, Zn(II) has a filled d^{10} orbital,[11] and as such it does not participate in electron transfer processes, resulting in fluorescence quenching. However, coordination of tpy units to Zn(II) ions blocks their free rotation, consequently reducing the quenching processes associated with it. This in turn results in the fluorescence enhancement of Zn–**L** assemblies.[13c–e]

The changes in the absorption and the fluorescence spectra were analyzed using nonlinear regression analysis.[14] The values of the binding constants are presented in Supporting Information Table S1. In the case of Fe(II) and Ni(II) the factor analysis suggested the presence of 3 or 4 absorbing/emissive species; the best fit being obtained when **L**, **ML**, and $\mathbf{M_3L_2}$ were used. The factor analysis for the titration with Cu(II) suggested the presence of 4 absorbing and 3 fluorescent species; the best fit indicating the successive formation of 1:1, 2:1, and 3:1 **M:L** species (Figure 3). For Zn(II) this analysis suggested the presence of 3 species for both data sets. The absorbance changes were best fit to the presence of **L** along with **ML** and $\mathbf{M_2L}$ assemblies in solution with surprisingly high binding constants.[15] The changes in the absorbance of **L** upon addition of Ru(III) were best fit to the formation of **ML**, $\mathbf{M_3L}$, and $\mathbf{M_3L_2}$ species while the changes in the fluorescence suggested the formation of **ML** and $\mathbf{M_3L_2}$ assemblies. This is a surprising result as Ru(III) normally forms more stable coordination complexes with mono-tpy ligands, while Ru(II) forms stable complexes with bis-tpy derived structures.[10e]

The formation of $\mathbf{M_3L_2}$ structures above may be explained by the formation of $\mathbf{L_2}$ dimers at the beginning of the ligand supramolecular polymerization process.[5a] This is an important interaction seen in ligands that are structurally related to **L** and can self-assemble into one-dimensional helical stacks that are stabilized by hydrogen-bonding and π–π interactions. This assembly pathway eventually gives rise to formation of aggregates and gelation, which in the case of **L** can be further

DOI: 10.1021/acs.inorgchem.5b00626
Inorg. Chem. 2015, 54, 7735–7741

cross-linked by the addition of d-block ions. To investigate this, we formed gels of **L** and studied its morphology in both the "free" or non-cross-linked form, and upon treating the gel with 3 equiv of d-block ions. The ligand gel was formed in a mixture of H_2O/CH_3OH (70:30) solvents upon slow evaporation over a period of days when the concentration of **L** reached 0.3 wt % (Figure 1).[5a] SEM imaging demonstrated that the gel is soft and made up of a fibrous network with an average fiber width of ∼20−22 nm (Figure 5A and Supporting Information Figure S12), while electron diffraction patterns during TEM analysis suggested the formation of supramolecular polymer within the gel through extended 1D 3-fold hydrogen bonding between BTA units with distances of ca. 0.36 nm.[5a] The formation of metallogels using d-block metal ions as cross-linking points was achieved by addition of solution of the d-block metal ions in water to the preformed **L** gel. This allowed the ions to slowly diffuse through the gel structure, complexing to the tpy centers and cross-linking the fibrous network in the process. It can be clearly seen in Figure 1, for Cu(II) and Ru(III) gels, as upon complexing to tpy, concomitant color changes occurred, with Cu(II) giving rise to the formation of a green cross-linked metallogel. We also monitored the diffusion of Fe(II) ions into the **L** gel over a period of time and the formation of the purple gradient that is typical of the formation of the visible MLCT-based absorption: the hallmark of the binding of Fe(II) to tpy and a clear indication of cross-linking self-assembly formation within the gel structure (Figure 5B, inset). Upon interaction of Fe(II) ions with **L**, the gel retained its fibrous structure with the width of the fibers appearing to increase to ∼40−50 nm, indicating the interaction of the ligand fibers through coordination of tpy units to metal ion linkers (Figure 5B). Furthermore, the Fe(II) cross-linked gel was stored at ambient conditions over a period of six months, and the oxidation of Fe(II) to Fe(III) was observed as the color of the gel changed from purple to orange-brown, demonstrating the sensitivity of the system to the presence of oxygen.

The morphology of Zn(II) gel, although being fibrous, indicated more significant deviation from the morphology of **L** gel with the average width of the fibers observed in the range ∼53−68 nm (Figure 5C). Here again the increase of the fibers width indicates the coordination of tpy antennae to Zn(II) ions. Upon interaction of **L** gel with Ni(II) (Figure 6A), the density of fibers packing on the silicon surface is significantly higher compared to **L** gel with the width of the fibers being ∼53−63 nm similarly to being previously observed for Zn-**L** gel. Ru(III)-based metallogels retain a fibrous structure with the width of the fibers being observed within a similar range of that for previous metallogels, ∼53−59 nm (Figure 6B). Finally, the morphology of Cu-**L** gel consists of densely packed fibers as can be seen from SEM data represented in Figure 7A. In order to further understand the influence of Cu(II) on the morphology of Cu-**L** gel, it was studied using SEM along with HAADF (high-angle annular dark field) STEM (scanning transmission electron microscopy) imaging (Figure 7B,C and Supporting Information Figure S13). This data confirmed fibrous structure of the gel with much higher value of the fiber width being in the range ∼120−137 nm. Closer examination of these fibers revealed that they in turn consist of fibers with width of ∼20 nm corresponding to the values obtained for **L** gel fibers. This again allowed us to reveal the role of metal ions in the formation of metallogel acting as "supramolecular glue" within its structure. The formation of the fibers with higher width in the case of Cu(II) suggests that the ion binds into three tpy units extending the fibrous network in three dimensions as the presence of $\mathbf{M_3L}$ species was found during self-assembly experiments in the solution (see above and Supporting Information Table S1). Moreover, metallogels were more robust as they have shown higher stability during imaging compared to **L** gel alone, demonstrating that the mechanical properties of the gel were affected upon using the d-block metal ions as cross-linking "supramolecular glue". Unlike Jung et al.[6b] we did not see the formation of spherical structures upon addition of Zn(II), which might be due to the fact that these authors formed their system by mixing **L** and Zn(II) in a 2:3 ratio and in their case the presence of Zn(II) disturbed the hydrogen bonding and $\pi-\pi$ interaction between **L** molecules inducing molecular aggregation into the horizontal direction by metal−ligand coordination. In contrast, we have added metal ions into the preformed ligand gel with the intention to keep the vertical interactions between the ligand molecules and only used outer tpy moieties coordinating to metal ions and linking strands together into larger fibrous networks, which was successfully proven by microscopy analysis of the resulting gels. Moreover, authors[6b] have used $DMSO:H_2O$ solvent mixtures in the formation of their gel-system as opposed to $CH_3OH:H_2O$ mixture as used here.

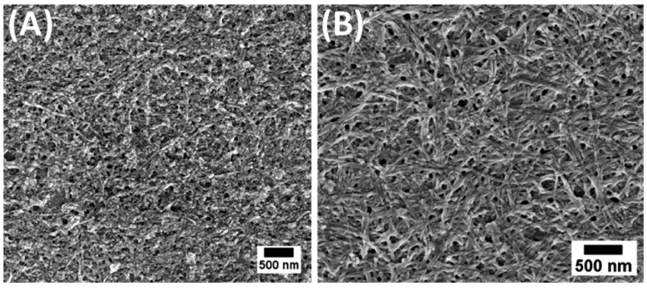

Figure 6. SEM images of (A) Ni(II)-**L** and (B) Ru(III)-**L** metallogels (scale bar corresponds to 500 nm). A very thin layer of gold/palladium was applied to enable imaging.

The optical properties of the investigated gels were recorded for the samples dried on the surface of microscope glass (see Supporting Information Figures S14 and S15). The absorption spectrum of **L** gels possesses a broad band centered at 325 nm, which corresponds to the tpy $\pi \rightarrow \pi^*$ transitions (Supporting Information Figure S14A). Upon Fe-**L** gel formation the appearance of the characteristic MLCT band was observed with a maximum centered at 570 nm, similar to the solution studies (see above and Supporting Information Figure S14B) and indicating the binding of tpy to Fe(II). The coordination of **L** to Ni(II) within the gel structure can be suggested as the maxima in the absorbance spectrum of Ni-**L** gel (Supporting Information Figure S14C), which is centered at 280, 310, and 330 nm and corresponds to the results from the self-assembly studies in CH_3OH solution (Figure 2B). At the same time the absorbance spectra of Cu-**L**, Zn-**L**, and Ru-**L** gels (Supporting Information Figure S14D−F) are broad and nonspecific, probably due to the presence of stacking interactions within the dried gel. Upon excitation at 280 nm only **L** and Zn-**L** gels were emissive, while the fluorescence of Fe-**L**, Ni-**L**, Cu-**L**, and Ru-**L** gels was quenched as previously discussed for solution studies (see above, Supporting Information Figure S15). The maximum of the **L** gel emission was observed at 464 nm and underwent a red shift compared to the fluorescence spectrum of **L** in CH_3OH solution at 1×10^{-5} M, most likely due to the

DOI: 10.1021/acs.inorgchem.5b00626
Inorg. Chem. 2015, 54, 7735−7741

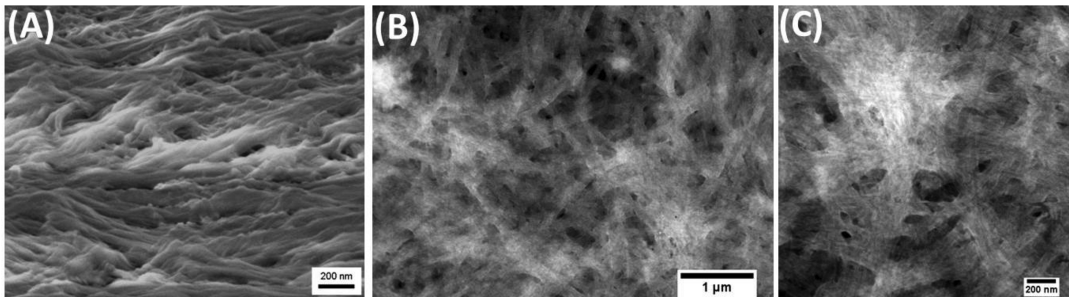

Figure 7. (A) SEM (scale bar 200 nm) and (B, C) HAADF STEM images of Cu(II)-**L** metallogel (scale bar for part B 1 μm and part C 200 nm), imaged at 80 kV with the gel manually deposited and dried as a thin film on a lacey-carbon TEM grid.

increased influence of interactions between ligand molecules at higher concentration of the gel. Similarly, the emission maximum for Zn-**L** was observed at 470 nm, which was again shifted to the red region of the fluorescence spectrum when compared with the self-assembled species between **L** and Zn(II) in the dilute solution. These results confirm binding interactions between tpy tripodal ligand and metal ions within the gel medium as well as the effect of the metal ions on optical properties of the resulting gels.

EXPERIMENTAL SECTION

Materials and Methods. All solvents and chemicals were purchased from commercial sources and used without further purification. Water was purified using a Millipore Milli-Q water purification system. Inorganic salts $FeCl_2{\cdot}4H_2O$, $NiCl_2$, $CuCl_2{\cdot}2H_2O$, $Zn(ClO_4)_2{\cdot}6H_2O$, and $RuCl_3{\cdot}H_2O$ were purchased from Aldrich. Mass spectrometry was carried out using HPLC grade solvents. Electrospray mass spectra were determined on a Micromass LCT spectrometer, and high-resolution mass spectra were determined relative to a standard of leucine enkephaline. Maldi-Q-Tof mass spectra were carried out on a MALDI-Q-TOF-Premier (Waters Corporation, Micromass MS technologies, Manchester, U.K.), and high-resolution mass spectrometry was performed using Glu-Fib with an internal reference peak of m/z 1570.6774.

Photophysical Measurements. All measurements were performed at 298 K in methanol solution (HPLC grade) unless otherwise stated. UV−vis absorption spectra were measured in 1 cm quartz cuvettes on a Varian Cary 50 spectrophotometer. Baseline correction was applied for all spectra. Fluorescence and excitation spectra were recorded on a Varian Cary Eclipse Fluorimeter. Quartz cells with a 1 cm path length from Hellma were used for these measurements. The temperature was kept constant throughout the measurements at 298 K by using a thermostated unit block.

In order to record absorbance and fluorescence spectra of the gels, a sample of gel was spread and then dried (at ambient conditions, 22 °C) on the surface of microscope glass slides (1 cm × 3 cm).

Spectrophotometric Titrations and Binding Constants. The formation of **M:L** species (where **M** = Fe(II), Ni(II), Cu(II), Zn(II), Ru(III); and **L** = terpyridine-based tripodal ligand) was ascertained by both UV−vis and luminescence titrations of a solution of **L** (1×10^{-5} M in methanol; concentration varied across experiments between 1.02×10^{-5} M and 1.05×10^{-5} M) with **M** (0 → 9 equiv). The data were fit using the nonlinear regression analysis program, SPECFIT.[14]

All of the inorganic salts were used to prepare $c \approx 5 \times 10^{-3}$ M stock solutions in Millipore water except $CuCl_2{\cdot}2H_2O$ and $Zn(ClO_4)_2{\cdot}6H_2O$ where methanol was used. These stock solutions were then diluted into methanol to the concentration of 1×10^{-3} M for the titration experiment.

Microscopy Studies of the Gels. For a view of the gel samples by scanning electron microscopy (SEM), samples were deposited manually onto clean silicon samples with a thick silicon dioxide layer. When using a spatula or glass pipet for dosing, the same cleaning procedure was used as for silicon substrates. All were cleaned thoroughly by sonication in HPLC grade acetone followed by HPLC grade propan-2-ol. They were then rinsed in ultrapure deionized water. All components were dried in two steps using first a high pressure nitrogen gun to blow away excess liquid and second an oven set at 80 °C to ensure removal of any trace solvent. The gels were manually drop cast onto the silicon once it returned to room temperature using clean micropipette tips or glass pipettes and spatulas as required. SEM was carried out using either the Zeiss ULTRA Plus in the Advanced Microscopy Laboratory, CRANN, Trinity College Dublin, or the Zeiss LEO 1430 VP at the Nanoscience Centre, University of Cambridge. No additional conductive coating was applied to aid imaging except where indicated in the text.

To prepare the Cu-**L** gel for analysis in the transition electron microscope (TEM), it was dosed to a lacey carbon support film in an Agar Scientific TEM copper grid. The sample was transferred to grids using a capillary contact transfer technique with a fine syringe needle. Samples were prepared at least a day in advance to allow sufficient time for the solvent to evaporate. The dry samples were stored under ambient conditions but were enclosed to protect against contamination. Samples were loaded directly into the microscope without further preparation steps and examined using the FEI Titan field emission TEM operated with an accelerating voltage of 80 keV for TEM and STEM analysis.

CONCLUSIONS

In conclusion, we have shown that tpy tripodal ligand **L** can be used for the formation of various metallogels with **M** = Fe(II), Ni(II), Cu(II), Zn(II), and Ru(III) at high ligand concentration. At the same time, the self-assembly processes at low concentrations of **L** were studied by monitoring the changes in its absorbance and fluorescence spectra upon gradual addition of **M** and the binding constants for the assembled species were determined and discussed. Optical and mass spectrometry studies clearly show the formation of **M-L** assemblies in solution and confirm the versatility of this system for biological and electronics applications, where the d-block metal ions are employed to add function to the ligand-based gel, clearly visible through both naked eye detection as well as through analysis of their resulting morphological properties. The addition of **M** to the preformed **L** gel shows that the gel retains its fibrous nature while increasing the width of the fibers by bringing 1D supramolecular polymers of **L**, formed through 3-fold hydrogen bonding between BTA, together through the interaction between tpy and d-metal ions. The presence of Zn(II) results in the formation of fluorescent gels while all the other metal ions quench fluorescence of **L**. We are currently investigating the application of these and related metallogels in greater detail especially focusing on the potential use as redox[16a−e] and fluorescence[16f] responsive gels.

DOI: 10.1021/acs.inorgchem.5b00626
Inorg. Chem. 2015, 54, 7735−7741

■ ASSOCIATED CONTENT

Supporting Information

Results of nonlinear regression analysis for the titrations performed and mass spectrometry analysis of **M-L** samples, SEM image of **L** gel, HAADF SEM images of Cu-**L** gel, the absorption and emission spectra of the **L** gel and its metallogels, and the table representing the binding constants obtained by fitting the titration data. The Supporting Information is available free of charge on the ACS Publications website at DOI: 10.1021/acs.inorgchem.5b00626.

■ AUTHOR INFORMATION

Corresponding Author

*E-mail: gunnlaut@tcd.ie.

Present Address

⊥Department of Chemistry, Durham University, Lower Mountjoy, South Road, Durham, DH1 3LE, UK.

Author Contributions

The manuscript was written through contributions of all authors. All authors have given approval to the final version of the manuscript. O.K., R.D., and C.M.G.d.S. contributed equally.

Funding

We thank Science Foundation Ireland for financial support in the form of a SFI PI 2010 (10/IN.1/B2999) and SFI PI 2013 (13/IA/1865) Grant (TG).

Notes

The authors declare no competing financial interest.

■ ACKNOWLEDGMENTS

Authors would like to thank Dr. Martin Feeney for mass spectrometry analysis and Dr. Markus Boese and the Advanced Microscopy Laboratory CRANN for imaging. We would like to thank Dr. Emma Veale for proofreading this manuscript.

■ REFERENCES

(1) (a) Pipenbrock, M.-O. M.; Lloyd, G. O.; Clarke, N.; Steed, J. W. *Chem. Rev.* **2010**, *110*, 1960−2004. (b) Kitagawa, S.; Kitaura, R.; Noro, S.-i. *Angew. Chem., Int. Ed.* **2004**, *43*, 2334−2375.

(2) (a) Leong, W. L.; Tam, A. Y.-Y.; Batabyal, S. K.; Koh, L. W.; Kasapis, S.; Yam, V. W.-W.; Vittal, J. J. *Chem. Commun.* **2008**, 3628−3630. (b) Braga, D.; d'Agostino, S.; D'Amen, E.; Grepioni, F. *Chem. Commun.* **2011**, *47*, 5154−5154. (c) Gee, W. J.; Batten, S. R. *Chem. Commun.* **2012**, *48*, 4830−4832. (d) Pipenbrock, M.-O. M.; Clarke, N.; Steed, J. W. *Soft Matter* **2010**, *6*, 3541−3547. (e) Pipenbrock, M.-O. M.; Clarke, N.; Steed, J. W. *Soft Matter* **2011**, *7*, 2412−2418.

(3) (a) *Functional Molecular Gels*; Escuder, B., Miravet, J. F., Eds.; The Royal Society of Chemistry: London, 2014. (b) Weiss, R. G. *J. Am. Chem. Soc.* **2014**, *136*, 7519−7530. (c) van Esch, J. H. *Langmuir* **2009**, *25*, 8392−8394. (d) Buerkle, L. E.; Rowan, S. J. *Chem. Soc. Rev.* **2012**, *41*, 6089−6102. (e) Aida, T.; Meijer, E. W.; Stupp, S. I. *Science* **2012**, *335*, 813−817. (f) Terech, P.; Weiss, R. G. *Chem. Rev.* **1997**, *97*, 3133−3159. (g) Estroff, L. A.; Hamilton, A. D. *Chem. Rev.* **2004**, *104*, 1201−1217.

(4) (a) Li, H.; Wu, L. *Soft Matter* **2014**, *10*, 9038−9053. (b) Tam, A. Y.-Y.; Yam, V. W.-W. *Chem. Soc. Rev.* **2013**, *42*, 1540−1567.

(5) (a) Kotova, O.; Daly, R.; dos Santos, C. M. G.; Boese, M.; Kruger, P. E.; Boland, J. J.; Gunnlaugsson, T. *Angew. Chem., Int. Ed.* **2012**, *51*, 7208−7212. (b) Cantekin, S.; de Greef, T. F.; Palmans, A. R. *Chem. Soc. Rev.* **2012**, *41*, 6125−6137. (c) Matsuura, K.; Murasato, K.; Kimizuka, N. *J. Am. Chem. Soc.* **2005**, *127*, 10148−10149. (d) Shen, Z.; Wang, T.; Liu, M. *Angew. Chem., Int. Ed.* **2014**, *53*, 13424−13428. (e) Daly, R.; Kotova, O.; Boese, M.; Gunnlaugsson, T.; Boland, J. J. *ACS Nano* **2013**, *7*, 4838−4845.

(6) (a) Jung, S. H.; Jeon, J.; Kim, H.; Jaworski, J.; Jung, J. H. *J. Am. Chem. Soc.* **2014**, *136*, 6446−6452. (b) Jung, S. H.; Kwon, K.-Y.; Jung, J. H. *Chem. Commun.* **2015**, *51*, 952−955.

(7) (a) Schubert, U. S.; Hofmeier, H.; Newkome, G. R. *Modern Terpyridine Chemistry*; Wiley-VCH: Weinheim, Germany, 2006. (b) Constable, E. *Chem. Soc. Rev.* **2007**, *36*, 246−253. (c) Chaurin, V.; Constable, E. C.; Housecroft, C. *New J. Chem.* **2006**, *30*, 1740−1744. (d) Vitvarová, T.; Zedník, J.; Bláha, M.; Vohlídal, J.; Svoboda, J. *Eur. J. Inorg. Chem.* **2012**, *2012*, 3866−3874.

(8) (a) Sénéchal-David, K.; Leonard, J. P.; Plush, S. E.; Gunnlaugsson, T. *Org. Lett.* **2006**, *8*, 2727−2730. (b) Nonat, A. M.; Allain, C.; Faulkner, S.; Gunnlaugsson, T. *Inorg. Chem.* **2010**, *49*, 8449−8456. (c) Byrne, J. P.; Kitchen, J. A.; Kotova, O.; Leigh, V.; Bell, A. P.; Boland, J. J.; Albrecht, M.; Gunnlaugsson, T. *Dalton Trans.* **2014**, *43*, 196−209. (d) Byrne, J. P.; Kitchen, J. A.; Gunnlaugsson, T. *Chem. Soc. Rev.* **2014**, *43*, 5302−5325.

(9) (a) Hu, C.-W.; Sato, T.; Zhang, J.; Moriyama, S.; Higuchi, M. *ACS Appl. Mater. Interfaces* **2014**, *6*, 9118−9125. (b) Sato, T.; Pandey, R. K.; Higuchi, M. *Dalton Trans.* **2013**, *42*, 16036−16042. (c) Gao, Y.; Rajwar, D.; Grimsdale, A. C. *Macromol. Rapid Commun.* **2014**, *35*, 1727−1740. (d) Chen, X.; Guo, K.; Li, F.; Zhou, L.; Qiao, H. *RSC Adv.* **2014**, *4*, 58027−58035. (e) Mehr, H. S.; Romano, N. C.; Altamimi, R.; Modarelli, J. M.; Modarelli, D. A. *Dalton Trans.* **2015**, *44*, 3176−3184. (f) Goldansaz, H.; Voleppe, Q.; Piogé, S.; Fustin, C. A.; Goju, J. F.; Brassinne, J.; Auhl, D.; van Ruymbeke, E. *Soft Matter* **2015**, *11*, 762−774.

(10) (a) Molloy, J. K.; Ceroni, P.; Venturi, M.; Bauer, T.; Sakamoto, J.; Bergamini, G. *Soft Matter* **2013**, *9*, 10754−10758. (b) Sambri, L.; Cucinotta, F.; De Paoli, G.; Stagni, S.; De Cola, L. *New J. Chem.* **2010**, *34*, 2093−2096. (c) Xiao, B.; Zhang, Q.; Huang, C.; Li, Y. *RSC Adv.* **2015**, *5*, 2857−2860. (d) Chen, X.; Huang, Z.; Chen, S.-Y.; Li, K.; Yu, X.-Q.; Pu, L. *J. Am. Chem. Soc.* **2010**, *132*, 7297−7299. (e) Ueki, T.; Takasaki, Y.; Bundo, K.; Ueno, T.; Saki, T.; Akagi, Y.; Yoshida, R. *Soft Matter* **2014**, *10*, 1349−1355.

(11) (a) Camerel, F.; Ziessel, R.; Donnio, B.; Guillon, D. *New J. Chem.* **2006**, *30*, 135−139. (b) Bhowmik, S.; Ghosh, B. N.; Rissanen, K. *Org. Biomol. Chem.* **2014**, *12*, 8836−8839. (c) Wang, R.; Geven, M.; Dijkstra, P. J.; Martens, P.; Karperien, M. *Soft Matter* **2014**, *10*, 7328−7336. (d) Bhowmik, S.; Ghosh, B. N.; Marjomäki, V.; Rissanen, K. *J. Am. Chem. Soc.* **2014**, *136*, 5543−5546. (e) Westcott, A.; Sumby, C. J.; Walshaw, R. D.; Hardie, M. J. *New J. Chem.* **2009**, *33*, 902−912.

(12) (a) Veale, E. B.; Kitchen, J. A.; Gunnlaugsson, T. *Supramol. Chem.* **2013**, *25*, 101−108. (b) Boyle, E. M.; Comby, S.; Molloy, J. K.; Gunnlaugsson, T. *J. Org. Chem.* **2013**, *78*, 8312−8319. (c) Comby, S.; Surender, E. M.; Kotova, O.; Truman, L. K.; Molloy, J. K.; Gunnlaugsson, T. *Inorg. Chem.* **2014**, *53*, 1867−1879. (d) Bradberry, S. J.; Savyasachi, A. J.; Martinez-Calvo, M.; Gunnlaugsson, T. *Coord. Chem. Rev.* **2014**, *273*−*274*, 226−241. (e) Caffrey, D.; Gunnlaugsson, T. *Dalton Trans.* **2014**, *43*, 17964−17970.

(13) (a) Ghosh, B. N.; Topić, F.; Sahoo, P. K.; Mal, P.; Linnera, J.; Kalenius, E.; Tuononen, H. M.; Rissanen, K. *Dalton Trans.* **2015**, *44*, 254−267. (b) Li, H.; Zhang, S.-J.; Gong, C.-L.; Li, Y.-F.; Liang, Y.; Qi, Z.-G.; Chen, S. *Analyst* **2013**, *138*, 7090−7093. (c) Albano, G.; Balzani, V.; Constable, E. C.; Maestri, M.; Smith, D. R. *Inorg. Chim. Acta* **1998**, *277*, 225−231. (d) Liang, L. J.; Zhao, X. J.; Huang, C. Z. *Analyst* **2012**, *137*, 953−958. (e) Hong, Y.; Chen, S.; Leung, C. W. T. L.; Lam, J. W. Y.; Liu, J.; Tseng, N.-W.; Kwok, R. T. K.; Yu, Y.; Wang, Z.; Tang, B. Z. *ACS Appl. Mater. Interfaces* **2011**, *3*, 3411−3418.

(14) (a) Gampp, H.; Maeder, M.; Meyer, C. J.; Zuberbühler, A. D. *Talanta* **1986**, *33*, 943−951. (b) Gampp, H.; Maeder, M.; Meyer, C. J.; Zuberbühler, A. D. *Talanta* **1985**, *32*, 95−101.

(15) Holyer, R. H.; Hubbard, C. D.; Kettle, S. F. A.; Wilkins, R. G. *Inorg. Chem.* **1966**, *5*, 622−625.

(16) (a) Kawano, S.-I.; Fujita, N.; Shinkai, S. *J. Am. Chem. Soc.* **2004**, *126*, 8592−8593. (b) Peng, F.; Li, G.; Liu, X.; Wu, S.; Tong, Z. J. *J. Am. Chem. Soc.* **2008**, *130*, 16166−16167. (c) Auletta, J. T.; LeDonne, G. J.; Gronborg, K. C.; Ladd, C. D.; Liu, H.; Clark, W. W.; Meyer, T. Y. *Macromolecules* **2015**, *48*, 1736−1747. (d) Zhang, Y.; Zhang, B.; Kuang, Y.; Gao, Y.; Shi, J.; Zhang, X. X.; Xu, B. *J. Am. Chem. Soc.* **2013**,

DOI: 10.1021/acs.inorgchem.5b00626
Inorg. Chem. 2015, 54, 7735−7741

135, 5008−5011. (e) Higuchi, M. *J. Mater. Chem. C* **2014**, *2*, 9331−9341. (f) Shao, H.; Wang, C.-F.; Zhang, J.; Chen, S. *Macromolecules* **2014**, *47*, 1875−1881.

DOI: 10.1021/acs.inorgchem.5b00626
Inorg. Chem. 2015, 54, 7735−7741